Environmental Research 236 (2023) 116603

Contents lists available at ScienceDirect

Environmental Research

journal homepage: www.elsevier.com/locate/envres

Dispersion of sneeze droplets in a meat facility indoor environment – Without partitions

Sunil Kumar [a], Mark Klassen [b], David Klassen [c], Robert Hardin [a], Maria D. King [a,*]

[a] Department of Biological and Agricultural Engineering, Texas A&M University, College Station, TX 77843, USA
[b] Canada Beef, Mississauga, ON, L5N 5R1, Canada
[c] Department of Mechanical Engineering, University of Calgary, Calgary, Alberta, T2N 1N4, Canada

ARTICLE INFO

Handling Editor: Jose L Domingo

Keywords:
COVID-19
Sneeze droplets dispersion
Computational fluid dynamics (CFD)
Indoor environment
Meat processing plant
Infection index

ABSTRACT

Spreading patterns of the coronavirus disease (COVID-19) showed that infected and asymptotic carriers both played critical role in escalating transmission of virus leading to global pandemic. Indoor environments of restaurants, classrooms, hospitals, offices, large assemblies, and industrial installations are susceptible to virus outbreak. Industrial facilities such as fabrication rooms of meat processing plants, which are laden with moisture and fat in indoor air are the most sensitive spaces. Fabrication room workers standing next to each other are exposed to the risk of long-range viral droplets transmission within the facility. An asymptomatic carrier may transmit the virus unintentionally to fellow workers through sporadic sneezing leading to community spread. A novel Computational Fluid Dynamics (CFD) model of a fabrication room with typical interior (stationary objects) was prepared and investigated. Study was conducted to identify indoor airflow patterns, droplets spreading patterns, leading droplets removal mechanism, locations causing maximum spread of droplets, and infection index for workers along with stationary objects in reference to seven sneeze locations covering the entire room. The role of condensers, exhaust fans and leakage of indoor air through large and small openings to other rooms was investigated. This comprehensive study presents flow scenarios in the facility and helps identify locations that are potentially at lower or higher risk for exposure to COVID-19. The results presented in this study are suitable for future engineering analyses aimed at redesigning public spaces and common areas to minimize the spread of aerosols and droplets that may contain pathogens.

1. Introduction

The Severe Acute Respiratory Syndrome Coronavirus 2 (SARS-CoV-2) also known as the causative agent of the COVID-19 pandemic, infected more than 645 million people, and already caused more than 6.6 million cumulative deaths across the globe as of December 11, 2022 (NCDC, 2022), since its emergence in December 2019. The spread of virus is caused by the infected as well as asymptomatic person without symptoms. The micron size droplets generated during coughs, sneezes, talks, and even breaths are emitted in the environment. Among respiratory events the sneeze is considered most violent, ejecting large numbers of saliva droplets of various sizes (Han et al., 2013), which can travel considerably long distances (Bourouiba, 2020) and feasibly deposit on closest surfaces (Asadi et al., 2020). The presence of contaminated droplets was observed on different surfaces. The probable survival of SARS-CoV-2 on various surfaces varies from few hours to days. COVID-19 virus can stay 4–5 days on paper, 4–9 days on plastics, up to 5 days on metals, up to 4 h on copper, 2–3 days on steel, up to 4 days on glass, up to 8 h on latex gloves, and 4–5 days on wood (Wiktorczyk-kapischke et al., 2021). A healthy person may get infected by touching these surfaces (secondary mode of transmission) accidently.

Studies have shown that the fate of the droplets primarily depends on their initial size (Wells, 1933; Xie et al., 2007). Large size droplets (>100 μm) fall under the effect of gravity, while small droplets (<100 μm) are easily affected by the surrounding airflow and can travel longer distance under the effect of airflow. The aerosolized droplets may keep floating for a long time and eventually evaporate into aerosol or droplet nuclei referred to as airborne transmission. Study by (Wells, 1933) showed that 100 μm droplets would settle on ground within 2 m, and up to 6 m, if sneeze jet velocity is 50 m/s (Xie et al., 2007). Exceptionally long traveled distance up to 8 m before losing its momentum has also been reported (Bourouiba, 2020), which is greatly affected by wind

* Corresponding author.
E-mail addresses: ksunil86.in@gmail.com (S. Kumar), mdking@tamu.edu (M.D. King).

https://doi.org/10.1016/j.envres.2023.116603
Received 20 December 2022; Received in revised form 26 June 2023; Accepted 7 July 2023
Available online 16 July 2023

localized airflow for indoor environments and wind speed for outdoors (Dbouk and Drikakis, 2020; Li et al., 2020).

One of the main reasons for accelerated spread of infection is interpersonal transmission of contaminated droplets, which may carry viral RNA via air route primarily (Asadi et al., 2020; Jayaweera et al., 2020; Tellier et al., 2019) and the other is the concentration of pollutants. The role of pollutants in the air on public health was investigated by many researchers. A comprehensive review study performed by (Domingo et al., 2020) assessed relationship between air pollutants concentration on airborne transmission of SARS-CoV-2 among the patients infected by coronavirus. The severely infected patients with the SARS-CoV-2 virus have the risk of developing the lethal form of COVID-19, specifically when they have a history of exposure to air pollutants such as sulfur oxides, nitrogen oxides, carbon monoxide and dioxide, particulate matter (PM), ozone and volatile organic compounds. These patients will have a complicated/delayed recovery (Comunian et al., 2020). A review on effect of air pollutants on the transmission and severity of the respiratory viral infection presented by (Domingo and Rovira, 2020) further notes that the decrease in the number of deaths during the quarantine periods is a result of huge decrease in air pollution. This shows clear evidence that high concentration of pollutants in the local environment adversely affects the human respiratory system.

Apart from the outdoor environment, the indoor environment of buildings is crucial for controlling the spread of respiratory infection (Passos et al., 2021) showed that small size droplets facilitate diseases including COVID-19 transmission through aerosolization. The swab sample from air exhaust grill also tested positive testifying that indoor airflow transported the droplets on vents (Ong et al., 2020). The study conducted by Zhou et al. (Zhou and Ji, 2021) investigates the influence of vortices generated in a fever clinic room on the transport of aerosols. The findings highlight that the position of stationary objects, such as the patient's bed, significantly alters the airflow patterns within the room. This observation suggests that the dispersion of droplets is highly sensitive to the position of the patient. (Kumar and King, 2022) performed a comprehensive study to show that the location of the diffuser is critical for achieving early decontamination of a hospital room. Placing the exhaust on the wall behind the patient and diffuser on the roof helps achieve early decontamination. Additionally, installation of a low flow air curtain further accelerates the decontamination even when small size droplets are uniformly diluted. In their review paper (Nair et al., 2022) discuss strategies aimed at mitigating indoor airborne transmission and enhancing air quality. One of the recommended approaches highlighted in the study is the implementation of negative pressure mix ventilation in hospital isolation rooms. Large size indoor environments of hospital areas (Grimalt et al., 2022), coach buses (Luo et al., 2022), slaughter facilities (Beck et al., 2019), and industrial installations are susceptible to virus outbreak. These large indoor spaces are subjected to thermal stratification (Wang et al., 2021), which refers to the development of layers of different temperatures (Kumar et al., 2017a, 2018). Thermal stratification is beneficial for a few systems (Gil et al., 2010), while performance could be deteriorating for critical systems (Kumar et al., 2017b, 2020a, 2020b, 2022). In a stratified indoor environment, the droplet nuclei may get trapped at certain height and can get transmitted over long horizontal distances. The initial size of the droplets determine the lock-up height in the stratified indoor environment (Liu et al., 2020, 2021).

The study conducted by Zhang et al. (2022) investigated the impact of environmental factors commonly observed in critical facilities, such as meat processing plants, on the interaction between the SARS-CoV-2 virus and its surroundings. These factors include low temperature, high humidity, and the presence of fatty acids. The study finds that these specific conditions significantly enhance the affinity of the virus for hydrophobic surfaces. Consequently, conventional sanitation methods like ventilation and hosing face challenges in effectively eliminating the virus, as the increased attachment prolongs its persistence on surfaces. Moreover, the study suggests that environmental conditions play a role in the transmission of SARS-CoV-2. Notably, airborne fat particles can facilitate the binding between the spike protein of the virus and fat aerosols, thereby enabling airborne transmission over greater distances. It is important to note that while close contact and respiratory droplets remain the primary modes of COVID-19 transmission, the presence of moisture and fat in the air has the potential to enhance the survival and transport of the virus in specific settings, particularly enclosed spaces. Therefore, a careful analysis to understand the routes of micron size droplets transmission under the effect of indoor airflow pattern is critically important.

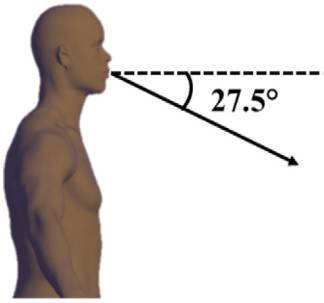

Fig. 1. Schematic diagram sneezer. The arrow indicates the reference inclination of the sneeze jet from the horizontal.

In the present study, an actual fabrication room (with a capacity of 116 workers) of a meat facility was investigated for the dispersion of sneeze droplets generated from seven different locations. CFD analysis helps understand the flow patterns developed in the fabrication room in the presence of stationary objects. The role and influence of large-scale vortices are assessed and analyzed in relation to the dispersion behavior of droplets, with the aim of establishing correlations between the presence of these vortices and their impact on droplet dispersion dynamics. The characteristics of the dispersion pattern provide crucial information to identify areas with risk of high and low exposure in the facility, where use of protective equipment would be especially helpful. Droplets removal mechanisms such as evaporation, deposition, and escape were investigated to understand the impact of airborne droplets. The detailed infection index for all the workers including stationary objects provides critical information for their safety. This study focuses on the characterization of indoor environment, and it could be extremely helpful for the safety teams, especially for the heating, ventilation, and air conditioning (HVAC) engineers. Based on the study, appropriate decontamination strategies can be developed.

2. Methods

Sneeze is a critical mechanism in which large pressure variation within a small period creates a fast flow in the upper respiratory tract, which breaks the saliva and mucus into small sized droplets that get sprayed from the mouth cavity. The ejection of sneeze ejecta is recognized as a transient mixture consisting of both droplets and exhaled air. Research conducted by (Busco et al., 2020; Gupta et al., 2009) demonstrates that the pressure response plays a key role as a time-varying parameter in comprehending the spraying of micron-sized droplets during the act of sneezing. For simulations, it was considered that an asymptotic worker expels a downward jet with a typical flow rate at an angle of 27.5° (Fig. 1).

2.1. Geometrical design of fabrication room

The photograph of the interior of the fabrication room considered for this study is shown in Fig. 2a. Typically, the fabrication room consists of central conveyer belts, fabrication tables, electric motor housings, and evaporators to circulate the cold air. A schematic diagram of the top and isometric view of the fabrication room including typical internals and

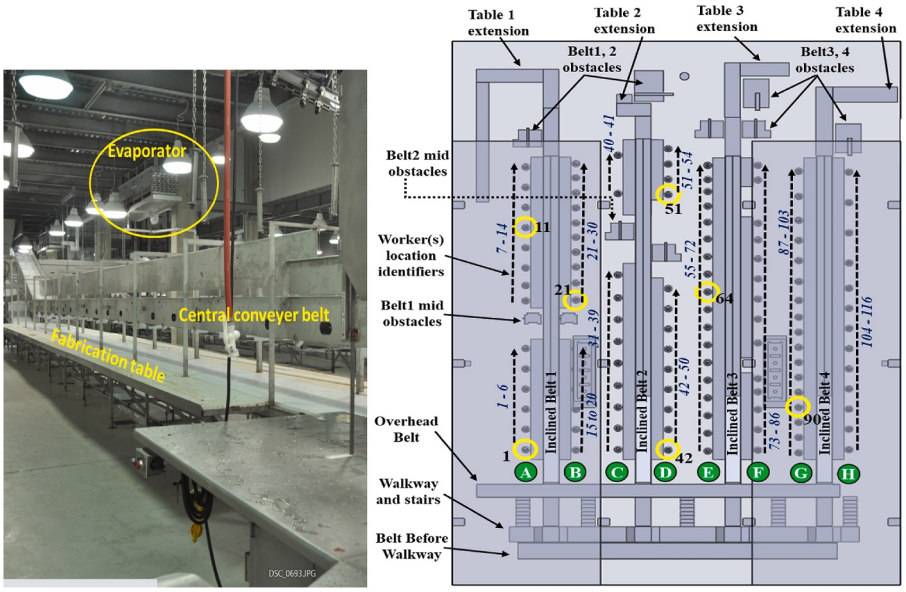

(a) (b)

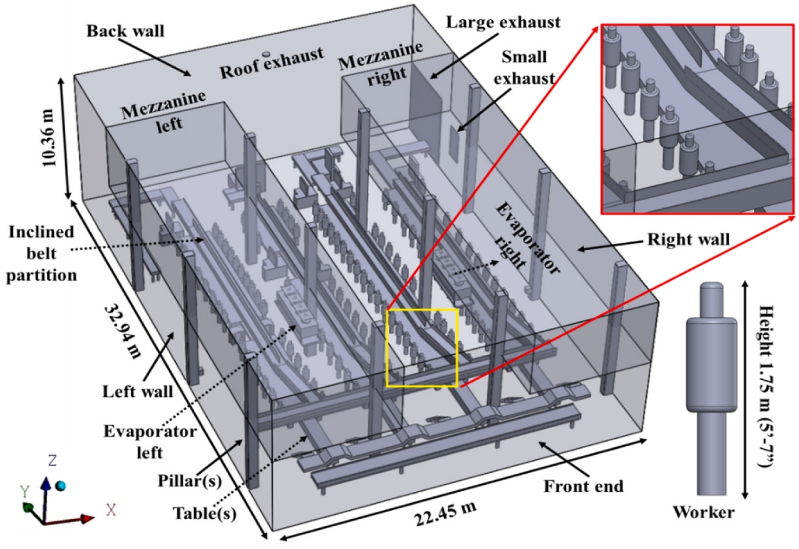

(c)

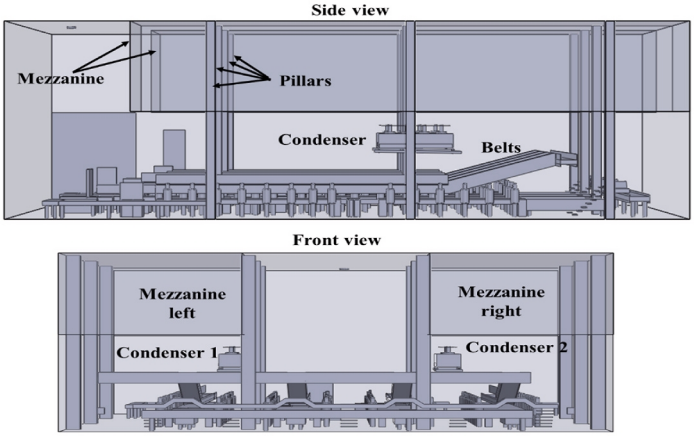

(d)

Fig. 2. (a) Inside photograph (b) Top view (c) isometric view, and (d) side and front views of fabrication room.

Table 1
Worker location identification number and assigned sneeze number.

Location	Sneeze number	Location	Sneeze number	Location	Sneeze number	Location	Sneeze number
64	Sneeze_S1	1	Sneeze_S2	42	Sneeze_S3	90	Sneeze_S4
21	Sneeze_S5	11	Sneeze_S6	51	Sneeze_S7		

workers standing at both sides of the table is shown in Fig. 2b (marked with yellow circles) and 2c. The workers are wearing protective apparel therefore appear like cylinder mannequins as shown in Fig. 2c. The workers are standing in columns A to H (numbered on green circles) as shown in Fig. 2b. The side and front views of the facility indicating pillars, mezzanine, condensers, and belts are shown in Fig. 2d.

The dimensions of the fabrication room along with the zoomed view of an area over the belt 3 are shown in Fig. 2c. Fresh air from the front end enters the facility. Indoor air is circulated mainly by the two evaporators at the left and right side. The exhaust on the roof, including the large and small units allows removal of ventilated air. Critical geometrical details of the internals of fabrication room were considered for the CFD modeling. Seven different sneeze locations selected to investigate droplets dispersion are highlighted by yellow circles and corresponding worker location identification numbers (Fig. 2b). Table 1 shows the worker location numbers and assigned sneeze numbers used for this study.

3. Numerical model

The Eulerian-Lagrangian approach is used to simulate the respiratory event of a sneeze. The dynamics of a single droplet resulting from a sneeze occur at a sub-grid scale, specifically within the computational grid. This sub-grid scale modeling approach is employed to approximate the influence of small-scale processes that are beyond the resolution capability of the grid. Pertinent parameters, such as the droplet's initial velocity, size, trajectory, and interaction with the surrounding airflow, are considered in the analysis. Moreover, crucial factors such as gravity, drag forces, and other relevant physical phenomena are accounted for. Through the utilization of appropriate mathematical models and equations, the simulation captures the intricate interplay between the droplet and the turbulent airflow within the indoor environment. This approach facilitates a comprehensive understanding of droplet dispersion, enabling accurate analysis of droplet spread. Additionally, the droplets interact with the resolved Eulerian macro-scales by exchanging mass, energy, and momentum. The droplets are simulated as discrete phase while air is simulated as continuous phase.

The continuous phase moist air is modeled as compressible homogeneous mixture of dry air and water vapor by solving the conservation equations for scalar variables representing mass fractions of species. The water vapor and air are assumed to share the same temperature, velocity, and pressure forming the homogeneous mixture. Interaction between droplets and moist air is achieved by interphase mass, momentum, and energy exchange. The Reynolds number used for peak sneeze velocity is 20000 (Busco et al., 2020).

The Lagrangian phase has two critical components namely "Droplet tracking" and "Droplet evaporation". Tracking is performed by integrating the force balance which is equated using inertia with forces acting on the droplet. Stochastic tracking is performed using Random Walk model and Random Eddy lifetime for each airborne droplet. Evaporation of the droplets is governed by the diffusive flux of the droplet vapor in the air. The presence of non-volatile components such as mineral salts lower the saturation pressure of water, which affects the droplets' evaporation rate. The vapor pressure of the saturated and pure water is used to calculate the activity coefficient, while Reynolds and Schmidt numbers are employed to calculate the mass transfer coefficient. Droplets temperature variation is governed by thermal balance including sensible and latent heat. Droplets distortion and breakup is accounted by Taylor Analogy Breakup (TAB) model (O'Rourke and Amsden, 1987). The equations pertaining to the numerical model utilized for conducting the simulations can be found in the Supplementary S8.

Table 2
Details of velocity and temperature boundary conditions.

Zone	Boundary condition	
	Temperature (°C)	Velocity (m/s) /Flow rate (kg/s)
Workers and Asymptomatic Sneezer	Constant Temperature (34 °C)	No slip ($u_x = u_y = u_z = 0$)
Walls, floor, roof, belts, tables, electric housings	Adiabatic ($\frac{\partial T}{\partial x} = \frac{\partial T}{\partial y} = \frac{\partial T}{\partial z} = 0$)	No slip ($u_x = u_y = u_z = 0$)
Imaginary wall air inlet	10 °C	$u_x = u_z = 0, u_y = 0.0135$
Evaporator inlet flow rate	–	4.42 (kg/s)
Evaporator outlet flow rate	2 °C	$u_x = u_y = 0, u_z = 9.04$
Roof exhaust	–	2.15 (kg/s)
Large exhaust	–	0.53 (kg/s)
Small exhaust	–	0.0589 (kg/s)

3.1. Model assumptions

For simulations the following assumptions were made:

1. The fresh, clean unidirectional air enters the fabrication room from the front end of the facility.
2. All the workers wearing protective apparel appear as cylindrical mannequins.
3. Internal objects of significant importance to airflow are modeled with simplification.
4. Workers marked in Fig. 2b sneeze away from conveyor belt in downward direction.
5. Workers are considered stationary for the duration of simulation.

3.2. Boundary conditions

For CFD simulations, all the walls including stationary objects were considered adiabatic. No slip boundary condition was imposed on all the surfaces including workers. The temperature and velocity boundary conditions are shown in table 2.

In the Eulerian-Lagrangian approach used to simulate respiratory event of sneeze, droplets interact with the resolved Eulerian macro-scales by exchanging mass, energy, and momentum. The droplets are simulated as discrete phase while air is simulated as continuous phase as described earlier under the numerical model.

Additional details of numerical method along with equations adopted for present study can be found in the previous publication of (Kumar and King, 2022) and the (ANSYS Fluent User Guide; Fluent Theory Guide).

4. Mesh independency test and CFD simulation setup

Details of the mesh independency test and simulation setup are presented below:

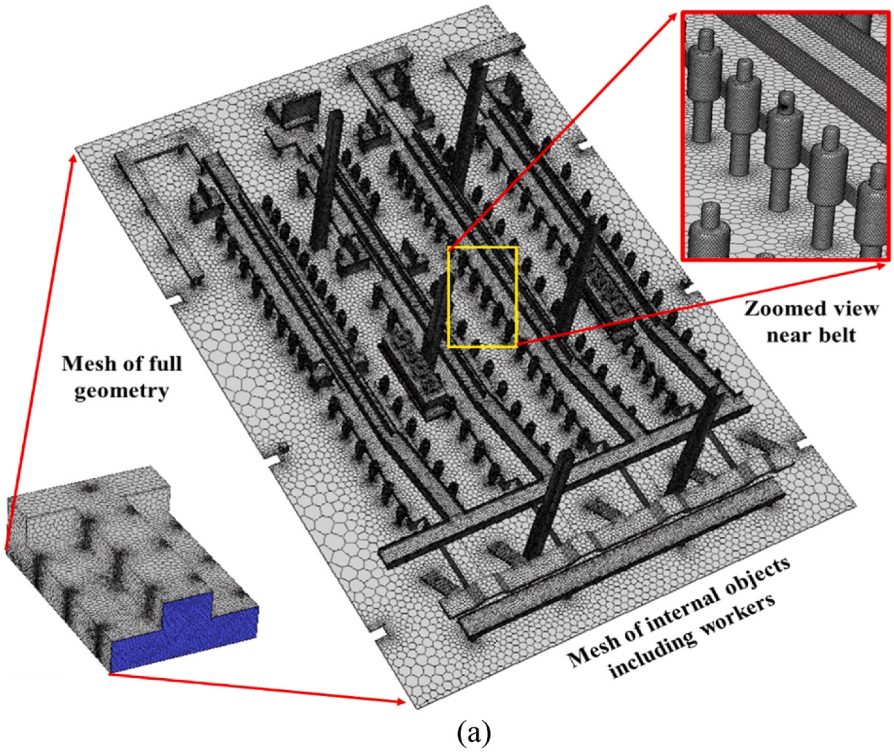

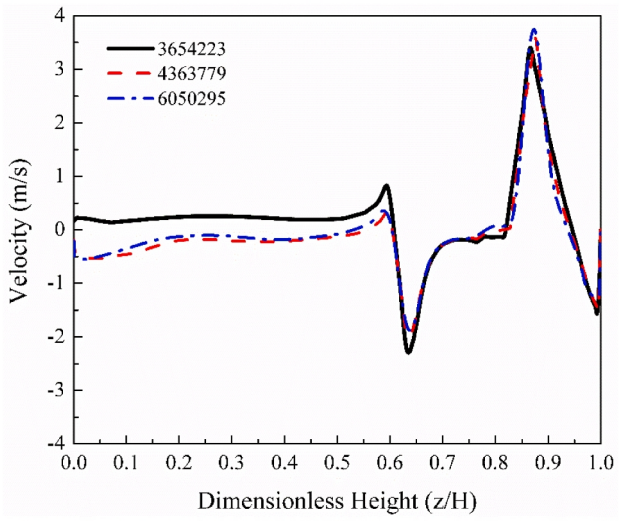

Fig. 3. Fabrication room (a) Meshed isometric view (b) velocity variation along the height.

4.1. Mesh independency test

The dimensions of the fabrication room are shown in Fig. 2c. The isometric meshed view of fabrication room, the mesh over workers and flow obstructions (e.g., conveyer belts, tables, electric housings, pillars, partitions, and inclined belts) and a zoomed view of an area over belt 3 are shown in Fig. 3a. The meshing was performed using polyhedral cells. A grid independency study was performed for the fabrication room. For the domain 3.65, 4.36, and 6.05 million cells were created. The mesh independency graph in Fig. 3b shows variation of velocity along the height of the fabrication room. The velocity for the mesh with 4.36 million cells behaves similarly to the mesh with 6.05 million cells and should have similar effects on droplets movement. Therefore, the mesh with 4.36 million cells was used for further simulations.

Table 3
Percentage error variation of velocity for different meshes.

z/H	Mesh 1 /Mesh 3	Mesh 2 /Mesh 3	z/ H	Mesh 1 /Mesh 3	Mesh 2 /Mesh 3
0.001	1.79	0.09	0.6	2.66	0.17
0.1	1.46	0.30	0.7	0.03	0.05
0.2	2.89	0.57	0.8	2.91	1.38
0.3	3.07	0.70	0.9	0.24	0.06
0.4	2.14	0.17	1.0	0.18	0.19
0.5	3.56	0.61			

Table 4
Direction of sneeze for asymptomatic sneezers.

Asymptomatic sneezer	X (radian)	Y (radian)	Z (radian)
Sneeze_S1	−1	−1	−0.48
Sneeze_S2	−1	1	−0.48
Sneeze_S3	1	1	−0.48
Sneeze_S4	−1	1	−0.48
Sneeze_S5	1	−1	−0.48
Sneeze_S6	−1	−1	−0.48
Sneeze_S7	1	−1	−0.48

A comparison of the percentage error in velocity variation for different meshes under investigation is shown in table 3. The error variation clearly indicates that 4.36 million cells are suitable for performing further simulations.

4.2. Details of simulation setup

In the present study, a pressure-based solver was employed for the simulations. The Realizable k-ε turbulence model, along with a scalable wall function and a y+ < 11, was utilized (Armand and Tâche, 2022; Jing et al., 2023; Santamaría Bertolín et al., 2023; Zou et al., 2018). The SIMPLE approach was used for pressure-velocity coupling. The second-order upwind scheme was used for density, momentum, turbulent kinetic energy, turbulent dissipation rate, and energy. The spatial discretization of pressure was implemented using a second-order scheme, which utilizes more information from the neighboring grid cells to calculate pressure gradients, resulting in improved accuracy in capturing pressure variations across the domain. For developing airflow in the facility, initially steady state simulations were performed, which were later used for transient simulations. The transient simulations were performed for 240 s (4 min), allowing sufficient time for droplets to spread and dilute in the room. Temperature and velocity data for the air inlet/outlet in facility are shown in table 2. For the simulations, an average humidity value of 68.5% was employed, determined through measurements using humidity sensors. It is important to note that humidity levels can fluctuate over time, and in consideration of this variability, an average value was chosen for the study. By using the average humidity value, the simulations aimed to provide a representative understanding of the system's behavior. In the present study, one single sneeze at a time from a designated sneezer shown in Fig. 2b and table 1 was considered for investigation. Sneeze droplets originate from a 2.25 cm^2 opening area and vary in size from 1 to 1000 μm, which is based on the experimental study by Han et al. (2013). For injecting droplets, the Rosin-Rammler diameter distribution approach (Bailey et al., 1983) was adopted with a mean diameter of 90 μm and a spreading parameter of 1.99 μm. A real sneeze is characterized by a mixture of water droplets entrained in the warm humid air from lungs in the direction as shown in table 4. Sneeze droplets were injected for a period of 0.2381 s (Busco et al., 2020) with a cumulative mass of 6.3 mg. Each droplet consists of 93.5% water and 6.5% salt in terms of mass fraction. The cough and sneeze show similar pressure responses with different intensities (Busco et al., 2020; Gupta et al., 2009).

Implemented sneeze velocity profile is based on previously published research by (Kumar and King, 2022) and obtained using the following equation-

$$v(t) = a_1\left(\frac{t}{c_1}\right)^{(b_1-1)} e^{\left(\frac{-t}{c_1}\right)} + a_2((t-d)/c_2)^{(b_2-1)} e^{\left(\frac{-(t-d)}{c_2}\right)} \text{ (m / s)} \quad (1)$$

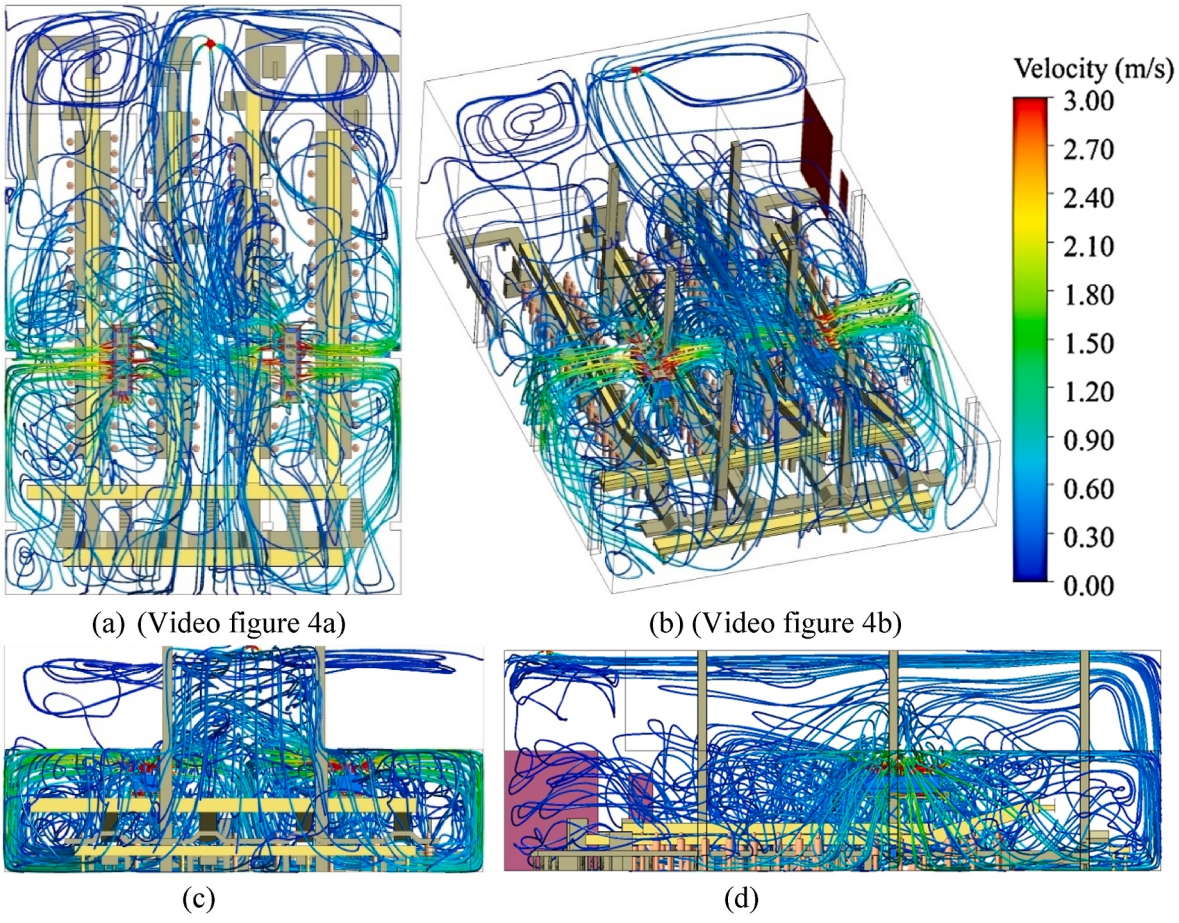

Fig. 4. Airflow streamlines (a) top view, (b) isometric view, (c) front view, and (d) side view in the fabrication room.

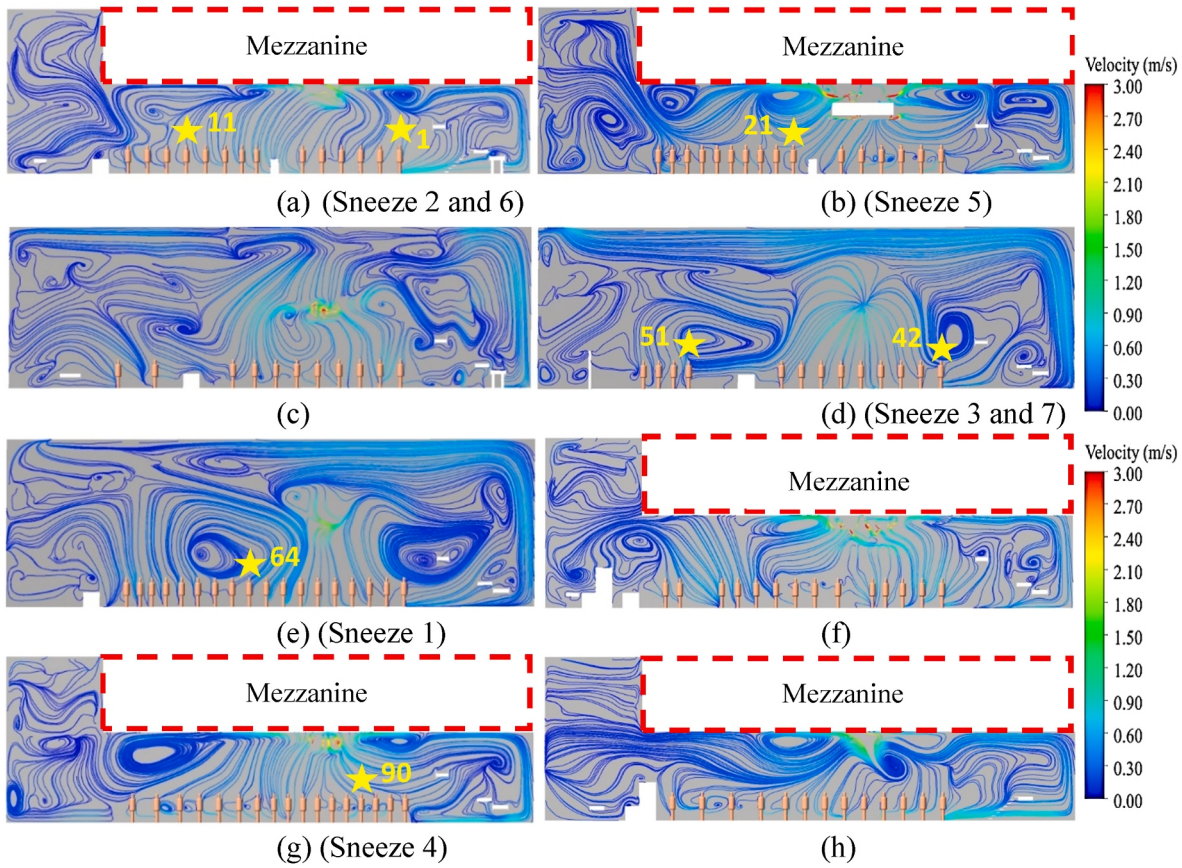

Fig. 5. Airflow streamlines in planes of (a) column A (left-most according to Fig. 2b), (b) column B, (c) column C, and (d) column D, (e) column E, (f) column F, (g) column G, and (h) column H, in fabrication room.

where the coefficients values are,

$a_1 = 12.7124$, $a_2 = -36.8307$, $b_1 = 5.7364$, $b_2 = 4.9688$, $c_1 = 0.0360$, $c_2 = 0.0373$, and $d = 0.0244$.

During exhalation, droplets and turbulent clouds were considered to have the same velocity. Sneeze droplets and air both at 38 °C exit the mouth cavity since the beginning of expiratory event. The droplets stop at 0.2381 s, while lung air continues to be exhaled up to 0.55 s. The droplet tracking accuracy of 10^{-5} was applied.

5. Validation of the evaporation model

Prior to conducting CFD simulations, a comprehensive validation of the droplet evaporation and fall from height models was performed using experimental data from the literature. The first validation case involved simulating the evaporation of a motionless droplet with a size of 1050 μm and an initial temperature of 25 °C in a dry environment at 9 °C, based on the experimental study by (Ranz and Marshall, 1952). Fig. S9a (available in Supplementary S9) shows transient variation of droplet diameter during the process of evaporation. In the second case, the variation in height and diameter of freely suspended droplets with sizes of 110 μm, 115 μm, and 170 μm in a humid environment (relative humidity 68%–70%) was validated against experimental studies conducted by (Hamey, 1982; Spillman, 1984). In Fig. S9b (available in Supplementary S9), the relationship between the height a droplet has fallen and the corresponding change in droplet diameter is shown. The validation of the model was performed using droplets of various diameters, at different initial temperatures, relative humidity values of the environment, and droplet temperatures. The CFD models demonstrated good agreement with experimental data from literature.

6. Results and discussion

The results obtained from the CFD study are discussed in the following sections.

6.1. Airflow velocity development and streamlines

The fabrication room consists of conveyer belts, tables, electric motor housing, extension tables and workers which all present obstructions for the airflow. Fresh air of 10 °C at 0.0135 m/s (equivalent to 4650 CFM) enters the fabrication room from the front end of the fabrication room. The indoor air is cooled and circulated by the two evaporators on left and right (Fig. 2). These evaporators blow cold air of 2 °C at 15000 CFM with the help of four air outlet fans on each as shown in Fig. 2c. The roof exhaust, with both the large and small exhausts allow the air to leave the fabrication room. Interactions of the air streams with walls, stationary surfaces and with each other develop a flow pattern as shown in Fig. 4.

Fig. 4a shows top, 4b shows isometric, 4c shows front and 4d shows side view of the airflow pattern in fabrication room. Overall flow pattern shows that the entire facility can be divided into four zones, with two small zones upstream and downstream of the evaporators. The airflow from the evaporator gets deflected towards the left and right walls, where a secondary deflection of airflow takes place. After secondary deflection, the major portion moves along the wall in downward direction and divides into two portions namely towards the front end and back wall of the facility (Fig. 4a,b and 4d).

Isometric view and side view show that the deflected air interacts with the incoming air (from the font end of facility) in the left zone before the left evaporator and creates large size circulation (Fig. 4b) of high activity. However, the area after both evaporators shows relatively

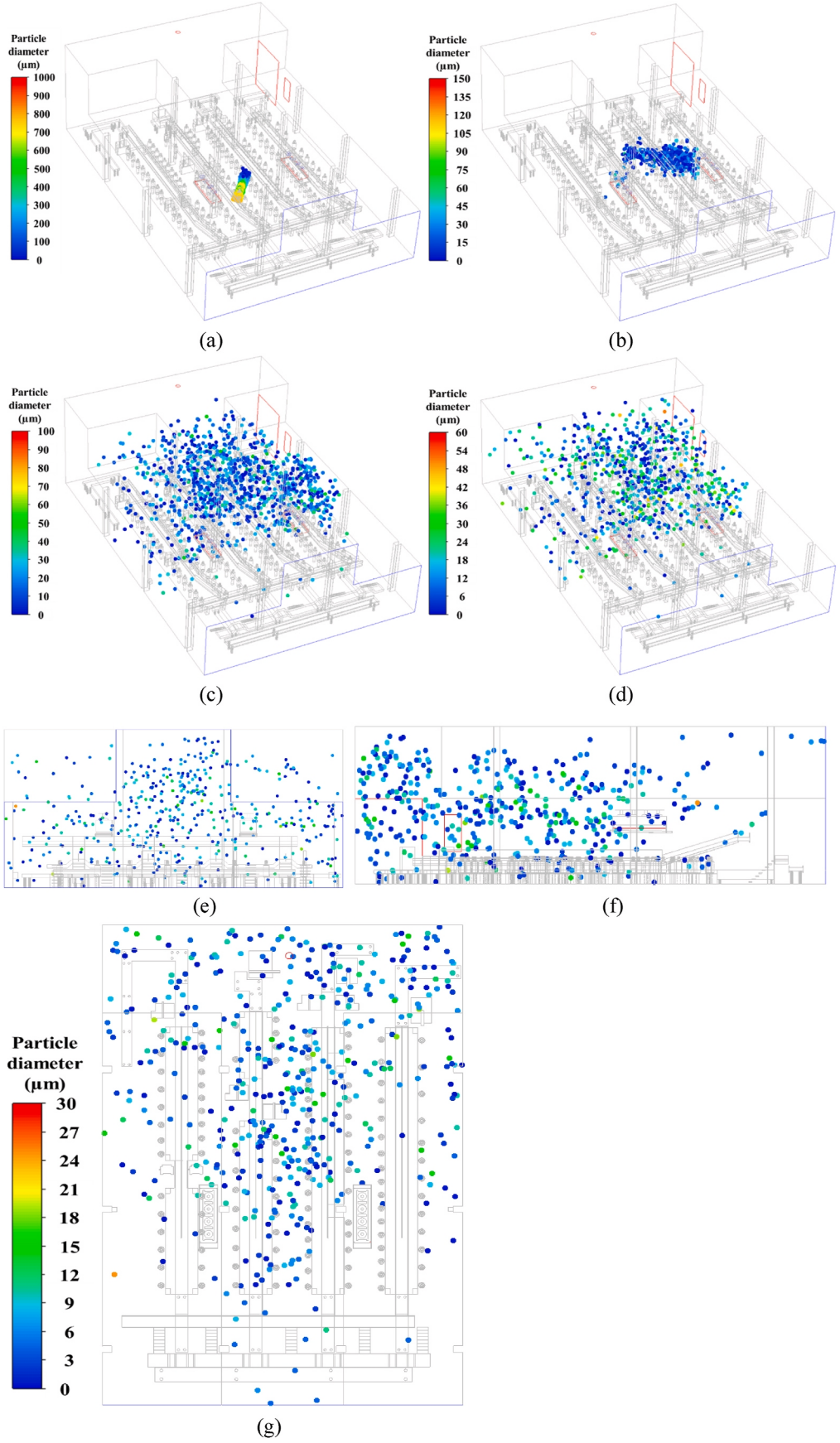

Fig. 6. Sneeze droplets dispersion for asymptomatic worker at location 64 (a) 0.5 s, (b) 15 s, (c) 115 s, (d) 155 s, (e) front, (f) side, and (g) top view at 240 s. Droplets dispersion video for this location is available at following link Sneeze_S1.

less air activity. The gap between the mezzanines behaves like a duct and allows development of long-range streamlines near the roof (Fig. 4d). A comprehensive airflow distribution in the fabrication room can be identified through videos for Fig. 4a and 4b, for understanding the droplets dispersion patterns discussed in following sections. The vortices developed in planes of columns A to H (Fig. 2b) are shown in Fig. 5.

Supplementary video related to this article can be found at https://doi.org/10.1016/j.envres.2023.116603

The overhead mezzanine areas in columns A, B, F, G and H are denoted as red rectangles. Large size vortices developed in the fabrication room can circulate, and transport contaminants including droplets from one location to another. These vortices significantly increase the risk of resuspension of contaminants and transmission of airborne viral droplets. The seven different sneeze locations considered for this study are indicated by yellow stars and corresponding location identification numbers.

The air velocity vectors in the fabrication room are presented in the Supplementary Fig. S1. The velocity vectors help understand the long- and short-range transmission leading to the overall dispersion of droplets.

6.2. Droplets dispersion in fabrication room

The droplets dispersion in such complex facilities depends on the airflow pattern and location of the sneeze. Therefore, 7 distinct locations (characterizing the entire fabrication room) were selected to release a sneeze by an asymptomatic worker, discussed in the following sections.

6.2.1. Asymptotic sneezer in column "E" at location 64 (Sneeze_S1)

In this case, it was considered that asymptotic worker is standing in column "E" at location 64 as shown in Fig. 2b. The worker sneezes downward directing droplets toward the floor of the fabrication room, as shown in Fig. 6a at 0.5 s. The sneeze droplets ejected in the indoor environment are subjected to deposition, escape, and evaporation processes. Deposition and escape processes completely remove the droplets from indoor environment, while evaporation processes decrease the mass of droplets making them susceptible to becoming airborne, which applies for all other sneeze locations also.

A complete sequence of droplets cloud dispersion from location 64 (past the evaporators) can be seen in the Sneeze_S1 video. Following the initial momentum, large size droplets (>500 μm) almost immediately deposit on the floor as can be seen for a duration of 0–3 s in the video. Simultaneously, medium (100–500 μm) and small size droplets (<100 μm) lose their momentum during flight and change their directions following the airflow streamlines. The availability of the mezzanine gap over the workers provides enough space to develop a large vortex capable of transferring droplets in the fabrication room. Upward rising droplets cloud (Fig. 6b) influenced by the combined airflow effect of both evaporators attempts to pull the droplets towards left, right and back side wall following the streamlines (Fig. 4a and 4b). However, Fig. 6c shows that the majority of the droplets are pulled towards the right wall, since location 64 is positioned geometrically towards the right side of fabrication room. The droplets reaching the gap between the mezzanines are pushed by long range streamlines towards the vortices past the evaporators near the back wall of the facility (Fig. 6d). Droplets distribution shown in Fig. 6e, 6f, and 6g for front, side, and top view indicates that droplets start diffusing towards the front end after filling the back side space of the facility.

Supplementary video related to this article can be found at https://doi.org/10.1016/j.envres.2023.116603

6.2.2. Asymptotic worker in column "A" at location 1 (Sneeze_S2)

For this case, the asymptomatic worker is standing in column "A" at location 1 (Fig. 2b). A complete sequence of droplets dispersion from location 1 can be seen in the video Sneeze_S2 and Supplementary Fig. S2. The worker sneezes downward directing droplets towards the floor (Fig. S2a). Large size droplets tend to deposit while medium and small size droplets tend to become airborne after losing their mass via evaporation. During their flight, loss of momentum causes a change in their direction, and droplets typically start to follow the streamlines. As shown in Fig. 4a and 4b, S1b and S1c, the air after secondary deflection from the walls moves toward the front end of fabrication room (videos of Fig. 4a and 4b). Air velocity remains high at around 1.8 m/s near the floor and relatively low near the mezzanine roof (Fig. S1). This effect is observable from Fig. S2b at 35 s, where large size droplets are pushed backward to become airborne along with small size droplets. These diffusing droplets are trapped in the lower left quadrant of indoor airflow distribution (Fig. 4a and S2c) and act as a source. The air circulation further resuspends these droplets of different sizes locally. The upward rising air at the center of fabrication room (Fig. 4d, and S2c) traps these droplets in the gap between the two mezzanines and starts spreading them in cleaner zones (Fig. S2d). Droplets distribution shown in Figs. S2e, S2f, and S2g for front, side, and top view indicates that the left section, specifically lower left quadrant of the fabrication room (Fig. 4a and S2d) remains highly contaminated posing a greater risk of exposure for workers.

Supplementary video related to this article can be found at https://doi.org/10.1016/j.envres.2023.116603

6.2.3. Asymptotic worker in column "D" at location 42 (Sneeze_S3)

For this case, the asymptomatic worker is standing in column "D" at location 42 (Fig. 2b). The worker sneezes downward towards the floor, as shown in Fig. S3a at 0.5 s. Droplets cloud dispersion can be seen from the video Sneeze_S3 and Fig. S3 in supplementary. In this case, after losing initial momentum and mass, droplets are pushed towards the front end of the fabrication room (Fig. S3b). This flow reversal towards the front end at the center of the facility is caused by the interacting cold air from both evaporators (Fig. S1). The relatively hot air (10 °C) entering from the front end of facility interacts with the cold air (2 °C) and generates large air circulation zones. Circulation of air over the column "D" at location 42 (Figs. 4 and 5d and S1) diffuses and stirs the droplets. Long range air streamlines (Fig. 5d) are able to transport the droplets to distant locations within 115 s (Fig. S3c). The streamlines deflection towards the width of fabrication room further diffuses droplets (Fig. S3d). Distribution of droplets at 240 s from the front, side, and top view (Figs. S3e, S3f, and S3g) shows that the sneeze released from location 42 is distributed uniformly after the initial concentration at the right side of facility.

Supplementary video related to this article can be found at https://doi.org/10.1016/j.envres.2023.116603

6.2.4. Asymptotic sneezer in column "G" at location 90 (Sneeze_S4)

For this case, the asymptomatic worker is standing in column "G" (almost below the evaporator on right) at location 90 (Fig. 2b). The worker sneezes towards the floor, as shown in Fig. S4a at 0.5 s. Droplets cloud dispersion can be seen from the video Sneeze_S4 and Fig. S4 in supplementary. Videos of Fig. 4a and 4b shows that the air from the surroundings and after second deflection from the right wall moves towards the inlet of the evaporator, and as a result the droplets cloud is strongly affected. The airborne droplets are strongly pulled by the right evaporator (Fig. S4b), resulting in the early escape of most droplets (Figs. S4c and S4d). Figs. S4e, S4f, and S4g for front, side, and top views respectively at 240 s show that the fabrication room is almost decontaminated, therefore presenting the least risk of spreading infection.

Supplementary video related to this article can be found at https://doi.org/10.1016/j.envres.2023.116603

6.2.5. Asymptotic sneezer in column "B" at location 21 (Sneeze_S5)

In this case, the asymptomatic worker is standing in column "B" (nearest to the evaporator on left) at location 21 (Fig. 2b). The worker sneezes towards the floor, as shown in Fig. S5a at 0.5 s. Droplets cloud

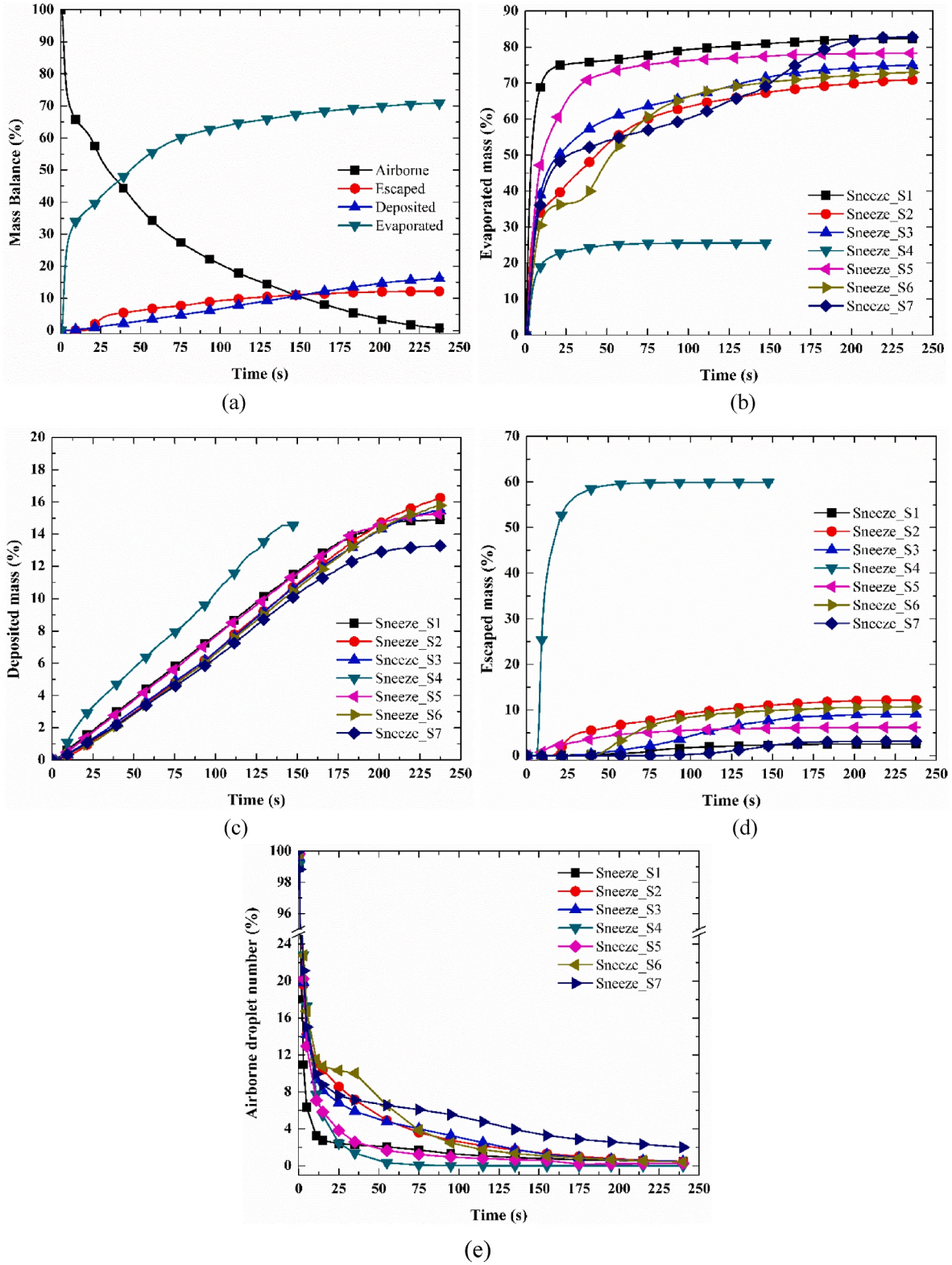

Fig. 7. Percentage of (a) mass balance for Sneeze_S2, (b) evaporated mass, (c) deposited mass and (d) escaped mass (e) airborne droplets number in fabrication room for different sneeze locations.

dispersion can be seen from the video Sneeze_S5 and Fig. S5 in supplementary. In reference to this location, airflow primarily takes place towards the left and back walls due to the bulk airflow from evaporator. The vortex created over the worker (Fig. 5b) is capable of transferring droplets from the cloud along the length of facility. On the other hand, the majority of the droplets cross over the inclined conveyer belt 1 and move towards the left wall, because of the localized flow along the width of facility (Figs. S5b and 4b). The secondary deflection of the airflow by the wall further divides these droplets into two groups in proportion of the airflow distribution (Fig. S5c).

Supplementary video related to this article can be found at https://doi.org/10.1016/j.envres.2023.116603

The vortex near the back wall of the facility (Fig. 5b) traps considerable number of droplets in the back portion in form of a cluster. While, droplets shifted towards the front end of facility, start diffusing like the sneeze at location 1 (figures S5c, S5d and S2c, S2d). Figs. S5e, S5f, and S5g for front, side, and top views respectively at 240 s show that the fabrication room is almost decontaminated, therefore presenting a lower risk of spreading infection. The droplets primarily accumulate over the inclined conveyer belts 1–3 and diffuse towards the right wall with time, thereby posing risk to the workers standing in column "H" as well.

6.2.6. Asymptotic sneezer in column "A" at location 11 (Sneeze_S6)

In this case, the asymptomatic worker is standing in column "A" at location 11 (Figs. 2b and 5a). The worker sneezes towards the floor as shown in Fig. S6a at 0.5 s. Droplets cloud dispersion can be seen from the video Sneeze_S6 and Fig. S6 in supplementary. Location 11 was selected to examine the behavior of droplets dispersion where the indoor air does not have the possibility to escape from any nearby exhaust and the sneezer is in a corner of the fabrication room. After initial deposition, the airborne droplets rise towards the mezzanine roof. The forward movement of droplets cloud is partially opposed by the local airflow, causing a few airborne droplets to be pushed backwards while the majority move towards the first quadrant of the facility (Fig. 4a and 4b) and (Fig. S6b and S6c). The droplets trapped in the first quadrant start dispersing like the sneeze that took place at location 1 (Figs. S6c and S2c). Figs. S6e, S6f, and S6g for front, side, and top view at 240 s show that droplets tend to diffuse in the fabrication room and the corner acts as droplets source.

Supplementary video related to this article can be found at https://doi.org/10.1016/j.envres.2023.116603

6.2.7. Asymptotic sneezer in column "D" at location 51 (Sneeze_S7)

In this case, the asymptomatic worker is standing in column "D" at location 51 (Figs. 2b and 5d). The worker sneezes towards the floor as shown in Fig. S7a at 0.5 s. Droplets cloud dispersion can be seen from the video Sneeze_S7 and Fig. S7 in supplementary. Location 51 allows to examine if recirculation of air can transport the sneeze droplets toward the front end of the fabrication room. After losing momentum, the airborne droplets cloud is captured by the local vortex over the worker (Fig. 5d), which starts pushing the droplets towards the center of facility (Fig. S7b). During this transfer, droplets are further exposed to opposing direction high airflow from the evaporators. Consequently, droplets quickly scatter in the back part of fabrication room (Figs. S7c and S7d) past the evaporators. Distribution of droplets in Figs. S7e, S7f, and S7g for front, side, and top view shows that droplets slowly diffuse towards the front end to dilute in the indoor air of the entire facility.

Supplementary video related to this article can be found at https://doi.org/10.1016/j.envres.2023.116603

Overall, it can be observed that droplets released by the workers standing around the inclined belts 1 and 2 will primarily spread in the left section of fabrication room. On the contrary, droplets released by workers standing around inclined belts 3 and 4 will spread in the right section of the fabrication room.

6.3. Factors affecting the removal of droplets from indoor environment

The sneeze droplets are subjected to escape, evaporation, and deposition depending on droplets size. Loss of droplets mass is governed by the initial droplet (38 °C) and surrounding air temperature difference. Large size droplets deposit under the influence of gravity. While small and medium size droplets deposit due to their momentum towards surfaces and walls. Loss of droplets due to escape is primarily dependent on streamlines, which terminate at exhaust. These processes lead to overall sneeze mass depletion from the fabrication room indoor environment. The fraction of deposited, evaporated, escaped and airborne mass can be calculated as-

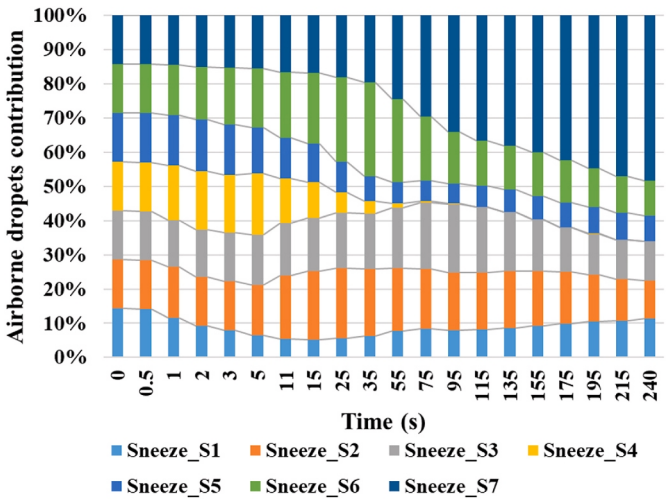

Fig. 8. Airborne sneeze droplets distribution for Sneezes 1 through 7 in fabrication room.

$$\text{Deposited mass } (\%) = \left(\frac{m_{deposited}}{m_{total}}\right) \times 100 \quad (2)$$

$$\text{Evaporated mass } (\%) = \left(\frac{m_{evaporated}}{m_{total}}\right) \times 100 \quad (3)$$

$$\text{Escaped mass } (\%) = \left(\frac{m_{escaped}}{m_{total}}\right) \times 100 \quad (4)$$

$$\text{Airborne mass } (\%) = \left(\frac{m_{airborne}}{m_{total}}\right) \times 100 \quad (5)$$

The transient mass loss balance in the fabrication room after sneeze by worker at location 1 in column "A" is shown in Fig. 7a. It was observed that around 50% of mass is depleted within the first 30 s. Evaporation is found to be the leading process for sneeze mass depletion (due to high droplet and room temperature difference) followed by deposition and escape. Since location 1 for sneeze_S2 is close to evaporator on the left, substantial droplets escape during rise of cloud initially. Later the dispersion of droplets, away from the evaporators, causes droplets to deposit more on different stationary surfaces including workers thereby increasing the overall deposition contribution. Similar depletion patterns were observed for other sneeze locations in the fabrication room.

A comparison of the evaporated, deposited, and escaped mass percentages for all sneeze locations is shown in Fig. 7b, 7c and 7d, respectively. Any droplet remaining airborne for a long time loses its mass mainly by evaporation. Fig. 7b and 7d shows that droplets originated by asymptomatic sneezer (Sneeze_S1) at location 64 in column "E" will mainly vanish by the evaporation process, with least contribution from the escape process. Similar effect can be seen for the asymptomatic sneezer in column "D" (Sneeze_S7) at location 51 (Fig. 7b and 7d). However, due to decreased deposition process after 180 s (Fig. 7c) large number of droplets remains airborne as seen in Figs. S7 and 7e. These airborne droplets quickly start dispersing towards the front end in the indoor environment.

The sensitivity of sneeze location can be distinctly seen for Sneeze_S4 at location 90 in column "G". The worker stands almost below the evaporator on the right side of fabrication room. Recirculating indoor air quickly pushes the upward rising sneeze droplets cloud towards the evaporator. As a result, 60% of the droplets mass escapes (Fig. 7d). Strong airflow activity in the surroundings of the sneezer causes escalated droplets deposition (Fig. 7c). Because droplets cloud spend least time after generation, therefore, evaporative loss is least for location 90

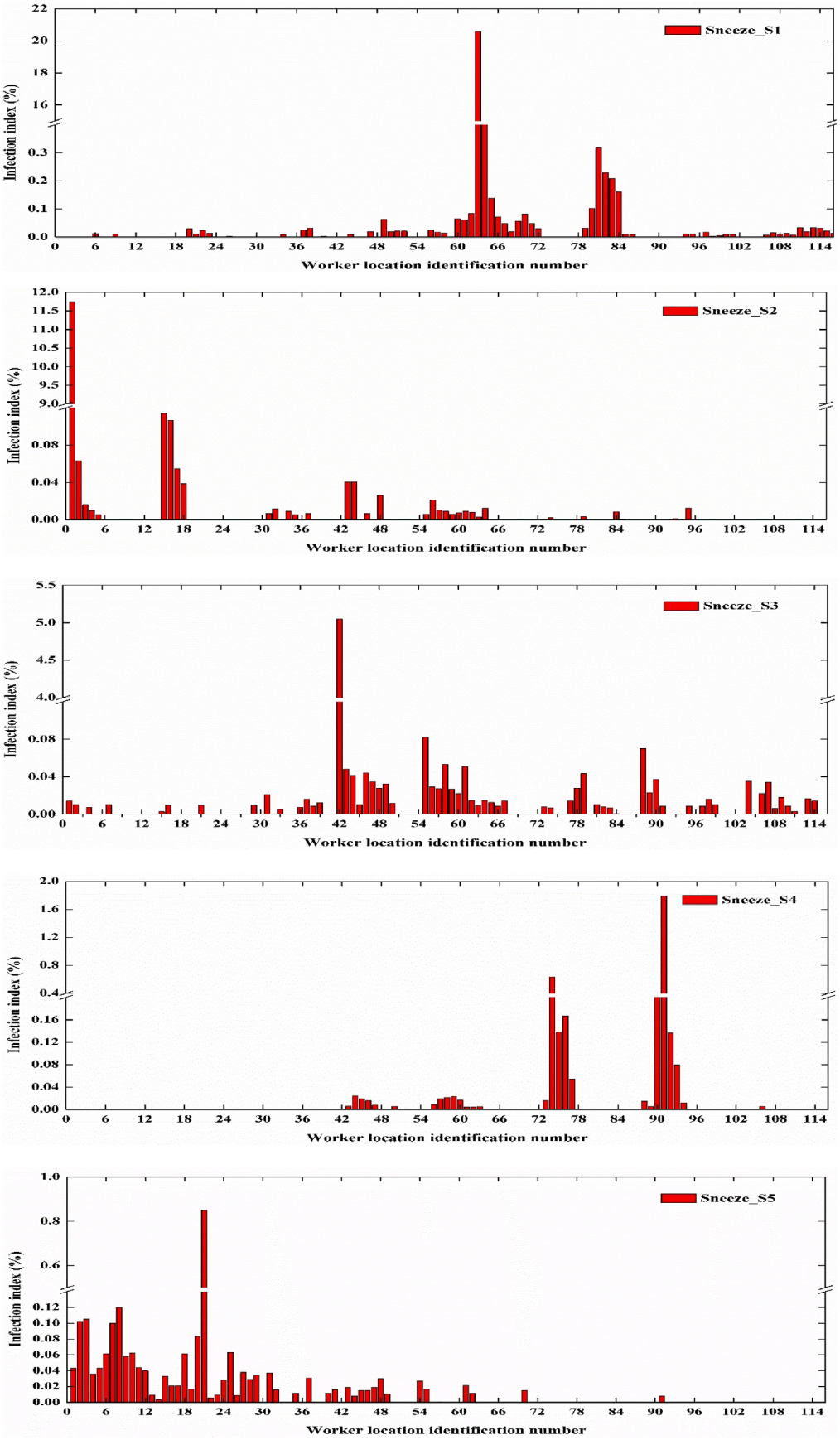

Fig. 9. Infection index for the workers in fabrication room corresponding to different sneeze locations.

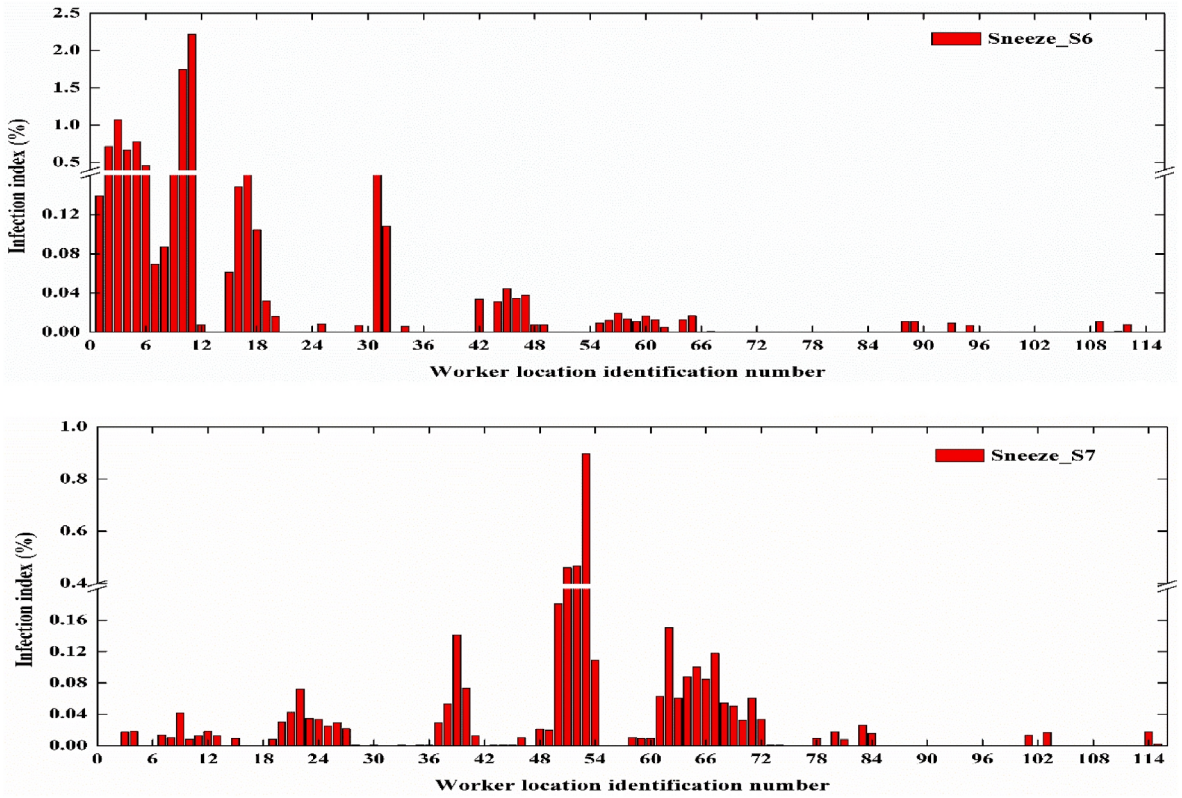

Fig. 9. (*continued*).

(Fig. 7b). As a result, droplets disappear from the indoor environment of fabrication room quickly.

The overall effect of different droplets removal processes on the fate of airborne droplets can be seen in Fig. 7e, which closely represents the effect of processes on airborne droplets for Sneeze_S7 after 240 s.

6.4. Relative presence of airborne droplets for different sneeze locations

Relative presence of airborne droplets at different time instants corresponding to different sneeze locations is shown in Fig. 8. They can be regarded independently for contributing to contamination of the indoor environment. It can be observed that droplets generated from location 90 (sneeze_S4) nearly vanish within 95 s compared to all others. A comparison of percentage airborne droplets variation at 240 s shows that the fabrication room has approximately the same percentage of airborne droplets when released from locations 1 (sneeze_S2), 42 (sneeze_S3), 21 (sneeze_S5), 64 (sneeze_S1), and 11 (sneeze_S6). However, when the sneeze takes place from location 51 (sneeze_S7), the fabrication room is exhibiting the highest number of airborne droplets. Therefore, location 51 would be highly contaminating for indoor environments of fabrication room type.

6.5. Effect of sneeze location on infection index

Long-range transport of the droplets with the help of indoor airflow pattern causes deposition of droplets over the workers and stationary objects in the entire fabrication room. Depending on the location of the sneeze, the workers and stationary objects are uniquely contaminated. Therefore, a healthy worker can directly or indirectly (by touching the solid surfaces) get infected. An infection index can be defined as the ratio of deposited mass on individual worker or surface(s) to total deposited mass.

$$\textit{Infection index}\ (\%) = \frac{\textit{Deposited mass on individual worker or surface}(s)}{\textit{Total deposited mass}} \times 100 \tag{6}$$

The location of workers in the fabrication room is marked from 1 to 116 and the names of stationary objects are shown in Fig. 2.

The infection index corresponding to different sneezes for all the workers in the fabrication room is shown in Fig. 9. A qualitative analysis for the "Sneeze_S1" shows that the surrounding workers at locations 60–67 and 80–84 get highly infected. Interestingly, neighboring worker 63 instead of sneezer at location 64 gets severely infected. For the "Sneeze_S2" it shows that worker 1 (sneezer), 2, 15–18 and 42–43 get most of infectious droplet's deposition. For the "Sneeze_S3", workers 42 (sneezer), 55, 58, 61, and 88 get most of infectious droplet's deposition. For the "Sneeze_S4", workers 90, 91 (sneezer), 92, 93 in the column "G" and nearby workers 73–76 also get infected. For the "Sneeze_S5", workers standing on both side in the beginning of inclined belt 1 get severely infected. Sneezer at location 21 gets highly infected. For "Sneeze_S6", workers 1–11, 15–18 and 31–32 in the column "A" and "B" get highly infected following the droplets dispersion patterns. For the "Sneeze_S7", workers 50–54, 61–70, and 38–40 including sneezer at location 51 get infected. All these infection index patterns strongly associate with indoor airflow (Figs. 4–5) and droplets dispersion (Fig. 6, S2-S7) patterns observed in previous sections.

Infection index for all the stationary indoor objects including walls of the fabrication room is shown in Fig. 10. A qualitative analysis shows that due to the direction of the sneeze, the floor of the fabrication room in all the sneezes becomes highly infected. Under the effect of airflow patterns infection index for floor can vary from 22% to 72%. Similarly, increased infection index can be observed for left and right-side evaporators depending on the relative distance of asymptomatic sneezer from either. A qualitative analysis for the "Sneeze_S4" clearly demonstrates that escape is the predominant process of droplets removal

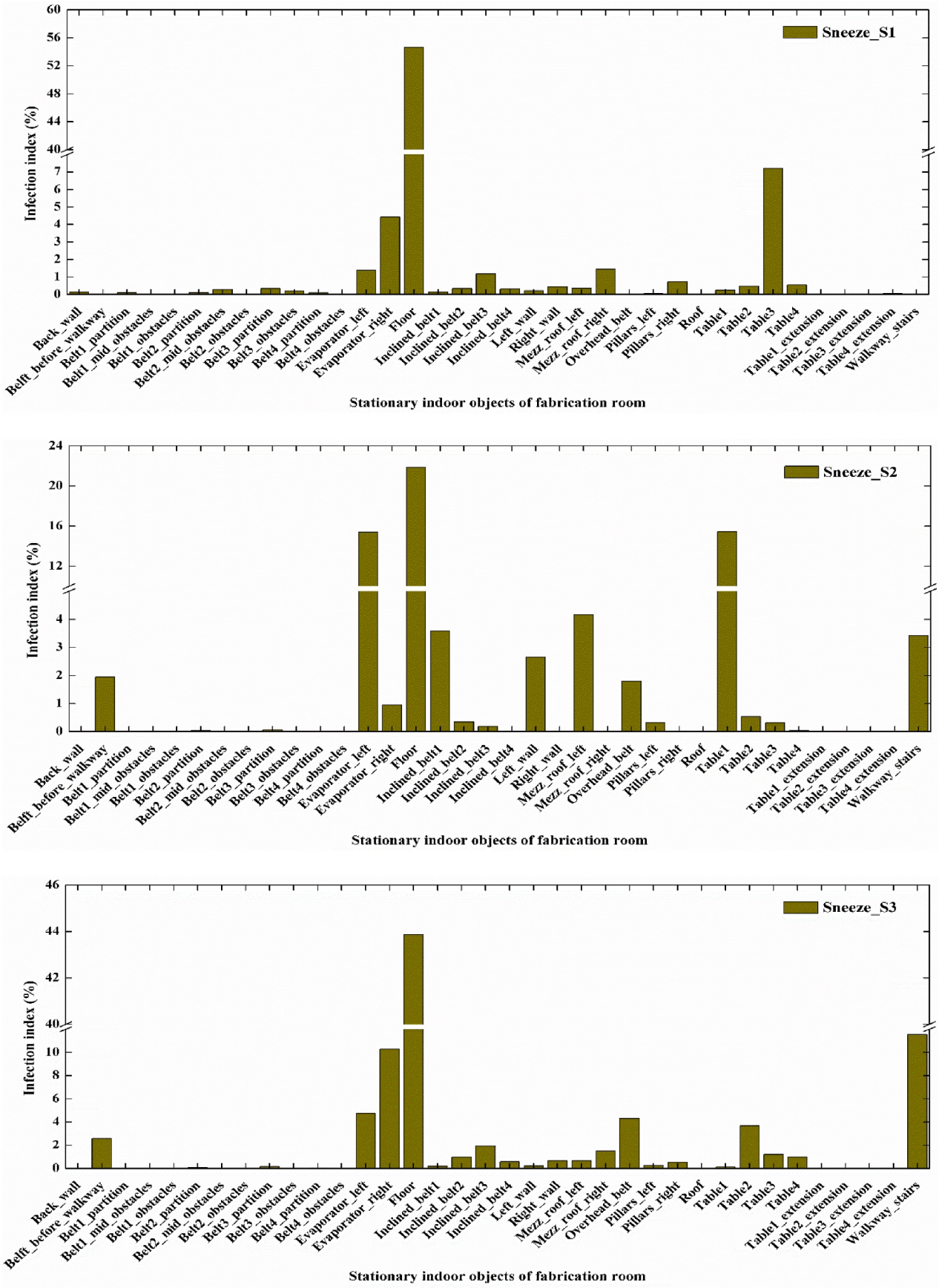

Fig. 10. Infection index for stationary objects present in the fabrication room corresponding to different sneeze locations.

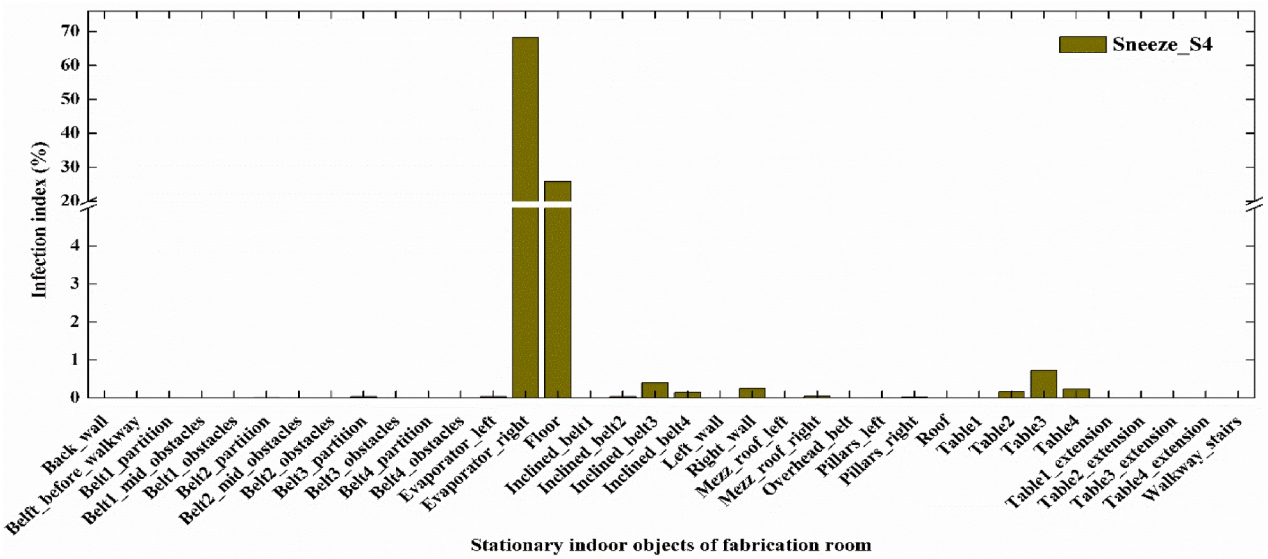

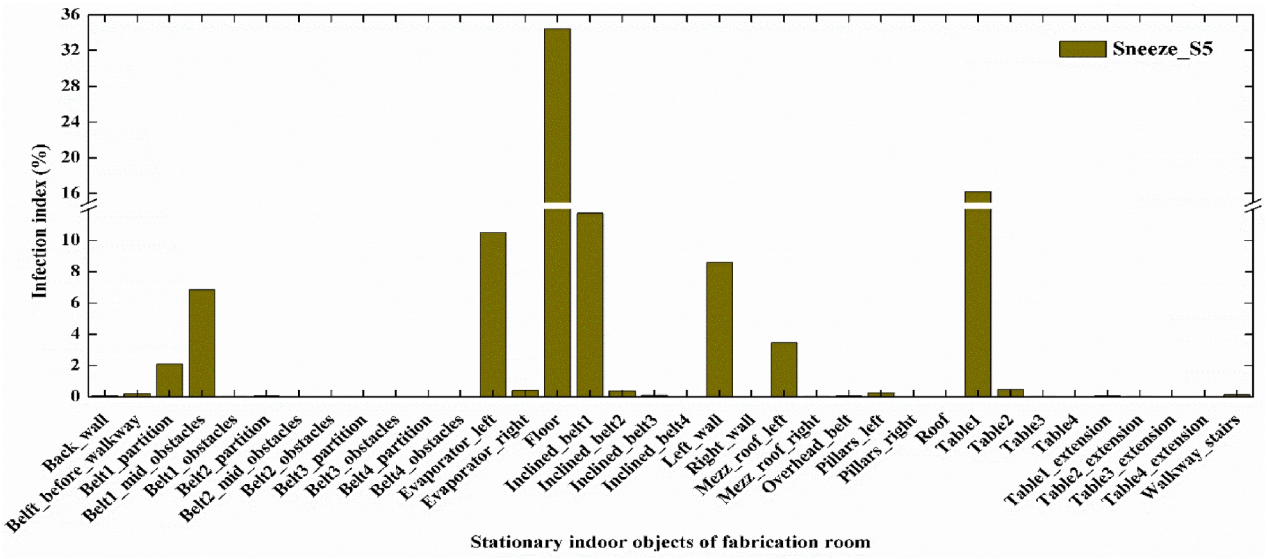

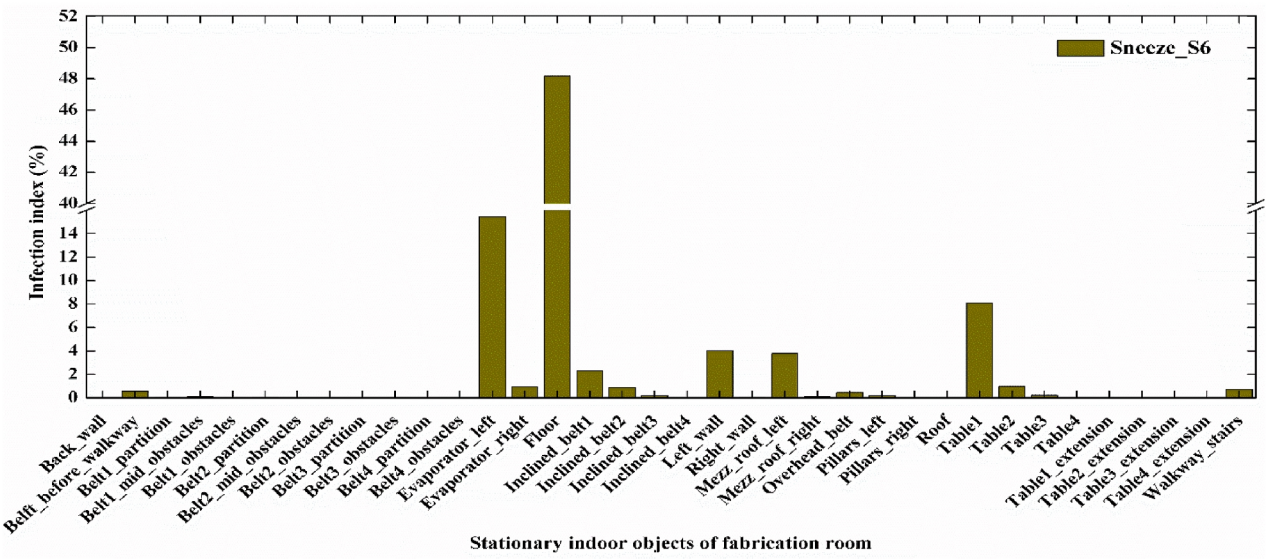

Fig. 10. (*continued*).

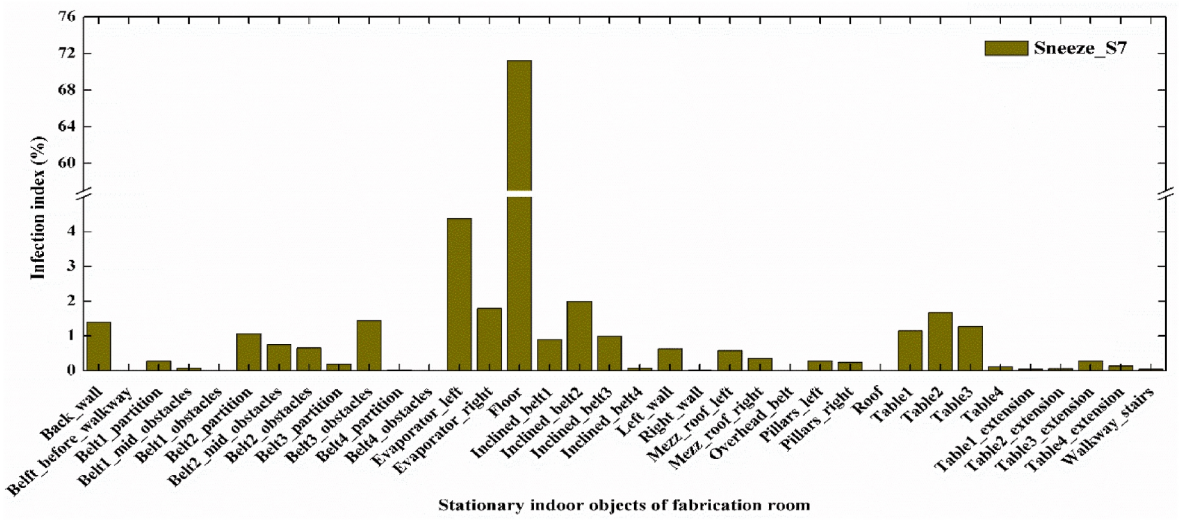

Fig. 10. (*continued*).

through the evaporator on the right. As a result, stationary objects in the fabrication room get least impacted, when sneeze is released from location 90 compared to all others. The infection indexes shown in Fig. 10 are found in close association with airflow and droplets dispersion patterns.

7. Conclusion

The indoor airflow pattern of all residential and commercial buildings depends on several factors including size of facility, stationary objects, location of diffuser and exhaust, number of occupants, ventilation rate, and location of evaporators (for commercial facilities). All the facilities with large occupants are highly vulnerable to the spread of airborne infections. Specifically, the fabrication rooms of meat facilities are highly susceptible to virus outbreak as indoor air is laden with moisture and fat particles. The airflow streamlines are capable of transporting contaminants and viral respiratory droplets generated by asymptomatic sneezer from remote locations. In this study, dispersion of sneeze droplets in fabrication room corresponding to selected sneeze locations is presented. The following conclusions can be drawn from the present study-

- The location of evaporators, exhausts, and stationary objects play a critical role in the development of unique airflow patterns. The reflected airflow from left and right walls each divide in two directions near the floor (Fig. 4).
- The complex airflow pattern primarily divides the whole fabrication room into four quadrants. Large size airflow vortices developed in the indoor environment consequently trap and spread the contaminated droplets.
- Respiratory droplets cloud strongly associate and follow the airflow pattern developed in the fabrication room.
- The location of the asymptomatic sneezer critically affects the droplets spreading behavior, which affects the decontamination processes. Sneeze_S4, by the asymptomatic sneezer at location 90 in column “G” is an excellent example.
- Evaporation remains the prevalent decontamination process followed by deposition and escape. Extended time spent by droplets cloud in air results in highest contribution to evaporation process.
- Sneeze_S7 by asymptomatic sneezer at location 51 in column “D” is found highly contaminating as droplets remain airborne for more than 240 s. While Sneeze_S4 by the asymptomatic sneezer at location 90 in column “G” supports early decontamination.
- The infection index for the workers as well as stationary objects is strongly correlated with the droplet’s dispersion pattern. The floor becomes highly infected for each sneeze location. Sneeze_S1 by asymptomatic sneezer at location 64 in column “E” causes neighboring worker 63 to have the highest infection index.

Results presented in this study are comprehensive and represent the entire fabrication room. It can be used to effectively model and mitigate the transmission of infectious diseases in large indoor environments. This study offers insight into designing appropriate decontamination measures.

Future studies include investigating the effects of partitions on droplets dispersion in fabrication rooms.

Credit author statement

SK conducted the simulations and analyzed and interpreted computational modeling and analysis data. MDK and SK designed the study, and both authors were major contributors to writing this manuscript. MDK and RH provided funding and critical discussions. MK and DK provided access to the facility and conducted measurements. All authors read and approved the final manuscript.

Declaration of competing interest

The authors declare that they have no known competing financial interests or personal relationships that could have appeared to influence the work reported in this paper.

Data availability

Data will be made available on request.

Acknowledgement

This work is a part of the NSF-CBET 2034048 award and the USDA National Institute of Food and Agriculture, Hatch project TEX09746 award. We thank the Texas A&M University High Performance Research Computing group (https://hprc.tamu.edu) for providing the computing resources.

Appendix A. Supplementary data

Supplementary data to this article can be found online at https://doi.

org/10.1016/j.envres.2023.116603.

References

ANSYS Fluent User Guide [WWW Document], n.d. URL.http://www.pmt.usp.br/academic/martoran/notasmodelosgrad/ANSYS Fluent Users Guide.pdf.

Armand, P., Tâche, J., 2022. 3D modelling and simulation of the dispersion of droplets and drops carrying the SARS-CoV-2 virus in a railway transport coach. Sci. Rep. 12, 1–22. https://doi.org/10.1038/s41598-022-08067-6.

Asadi, S., Bouvier, N., Wexler, A.S., Ristenpart, W.D., 2020. The Coronavirus Pandemic and Aerosols: Does COVID-19 Transmit via Expiratory Particles?, Aerosol Science and Technology. Taylor and Francis Inc. https://doi.org/10.1080/02786826.2020.1749229.

Bailey, A.G., Balachandran, W., Williams, T.J., 1983. The rosin-rammler size distribution for liquid droplet ensembles. J. Aerosol Sci. 14, 39–46. https://doi.org/10.1016/0021-8502(83)90083-6.

Beck, S.H., Castillo, A., Kinney, K.A., Zuniga, A., Mohammad, Z., Lacey, R.E., King, M.D., 2019. Monitoring of pathogenic bioaerosols in beef slaughter facilities based on air sampling and airflow modeling. Appl. Eng. Agric. 35, 1015–1036. https://doi.org/10.13031/AEA.13553.

Bourouiba, L., 2020. Turbulent gas clouds and respiratory pathogen emissions: potential implications for reducing transmission of COVID-19. JAMA 323, 1837–1838. https://doi.org/10.1001/JAMA.2020.4756.

Busco, G., Yang, S.R., Seo, J., Hassan, Y.A., 2020. Sneezing and asymptomatic virus transmission. Phys. Fluids 32, 1–18. https://doi.org/10.1063/5.0019090.

Comunian, S., Dongo, D., Milani, C., Palestini, P., 2020. Air pollution and covid-19: the role of particulate matter in the spread and increase of covid-19's morbidity and mortality. Int. J. Environ. Res. Publ. Health 17, 1–22. https://doi.org/10.3390/ijerph17124487.

Dbouk, T., Drikakis, D., 2020. On coughing and airborne droplet transmission to humans. Phys. Fluids 32, 053310. https://doi.org/10.1063/5.0011960.

Domingo, J.L., Marquès, M., Rovira, J., 2020. Influence of airborne transmission of SARS-CoV-2 on COVID-19 pandemic. A review. Environ. Res. 188, 17–20. https://doi.org/10.1016/j.envres.2020.109861.

Domingo, J.L., Rovira, J., 2020. Effects of air pollutants on the transmission and severity of respiratory viral infections. Environ. Res. 187, 109650 https://doi.org/10.1016/j.envres.2020.109650.

Fluent Theory Guide [WWW Document], n.d. URL.https://ansyshelp.ansys.com/account/secured?returnurl=/Views/Secured/corp/v201/en/flu_th/flu_th.html.

Gil, A., Medrano, M., Martorell, I., Lázaro, A., Dolado, P., Zalba, B., Cabeza, L.F., 2010. State of the art on high temperature thermal energy storage for power generation. Part 1—concepts, materials and modellization. Renew. Sustain. Energy Rev. 14, 31–55. https://doi.org/10.1016/j.rser.2009.07.035.

Grimalt, J.O., Vílchez, H., Fraile-Ribot, P.A., Marco, E., Campins, A., Orfila, J., van Drooge, B.L., Fanjul, F., 2022. Spread of SARS-CoV-2 in hospital areas. Environ. Res. 204 https://doi.org/10.1016/j.envres.2021.112074.

Gupta, J.K., Lin, C.H., Chen, Q., 2009. Flow dynamics and characterization of a cough. Indoor Air 19, 517–525. https://doi.org/10.1111/j.1600-0668.2009.00619.x.

Hamey, P.Y., 1982. The Evaporation of Airborne Droplets. Cranfield Institute of Technology.

Han, Z.Y., Weng, W.G., Huang, Q.Y., 2013. Characterizations of particle size distribution of the droplets exhaled by sneeze. J. R. Soc. Interface 10, 20130560. https://doi.org/10.1098/rsif.2013.0560.

Jayaweera, M., Perera, H., Gunawardana, B., Manatunge, J., 2020. Transmission of COVID-19 virus by droplets and aerosols: a critical review on the unresolved dichotomy. Environ. Res. 188, 109819 https://doi.org/10.1016/j.envres.2020.109819.

Jing, Y., Li, F., Gu, Z., Tang, S., 2023. Identifying spatiotemporal information of the point pollutant source indoors based on the adjoint-regularization method. Build. Simulat. 589–602. https://doi.org/10.1007/s12273-022-0975-z.

Kumar, S., Grover, R.B., Vijayan, P.K., Kannan, U., 2017a. Numerical investigation on the effect of shrouds around an immersed isolation condenser on the thermal stratification in large pools. Ann. Nucl. Energy 110, 109–125. https://doi.org/10.1016/j.anucene.2017.06.022.

Kumar, S., Grover, R.B., Yadav, H., Vijayan, P.K., Kannan, U., Agrawal, A., 2018. Experimental and numerical investigation on suppression of thermal strati fi cation in a water-pool : PIV measurements and CFD simulations. Appl. Therm. Eng. 138, 686–704. https://doi.org/10.1016/j.applthermaleng.2018.04.070.

Kumar, S., Grover, R.B., Yadav, H., Vijayan, P.K., Kannan, U., Agrawal, A., Grover, R.B., Kannan, U., Yadav, H., Agrawal, A., 2020a. Experimental investigations on thermal stratification in a large pool of water with immersed isolation condenser. Int. Conf. Nucl. Eng. Proceedings, ICONE 3, 1–7. https://doi.org/10.1115/ICONE2020-16647.

Kumar, S., King, M.D., 2022. Numerical investigation on indoor environment decontamination after sneezing. Environ. Res. 213, 113665 https://doi.org/10.1016/j.envres.2022.113665.

Kumar, S., Thyagarajan, A., Banerjee, D., 2022. Experimental investigation of thermal energy storage (TES) platform leveraging phase change materials in a chevron plate heat exchanger. In: International Mechanical Engineering Congress & Exposition, pp. 1–7. https://doi.org/10.1115/IMECE2022-96226.

Kumar, S., Thyagarajan, A., Banerjee, D., 2020b. An investigation on chevron plate heat exchanger filled with organic phase change material. In: Proceedings of the ASME 2020 Heat Transfer Summer Conference HT2020 July 13-15, 2020, Virtual. Online. American Society of Mechanical Engineers (ASME), pp. 1–6. https://doi.org/10.1115/HT2020-9122.

Kumar, S., Vijayan, P.K., Kannan, U., Sharma, M., Pilkhwal, D.S., 2017b. Experimental and computational simulation of thermal stratification in large pools with immersed condenser by. Appl. Therm. Eng. 113, 345–361. https://doi.org/10.1016/j.applthermaleng.2016.10.175.

Li, H., Leong, F.Y., Xu, G., Ge, Z., Kang, C.W., Lim, K.H., 2020. Dispersion of evaporating cough droplets in tropical outdoor environment. Phys. Fluids 32, 113301. https://doi.org/10.1063/5.0026360.

Liu, F., Qian, H., Luo, Z., Wang, S., Zheng, X., 2020. A laboratory study of the expiratory airflow and particle dispersion in the stratified indoor environment. Build. Environ. 180, 106988 https://doi.org/10.1016/j.buildenv.2020.106988.

Liu, F., Qian, H., Luo, Z., Zheng, X., 2021. The impact of indoor thermal stratification on the dispersion of human speech droplets. Indoor Air 31, 369–382. https://doi.org/10.1111/ina.12737.

Luo, Q., Ou, C., Hang, J., Luo, Z., Yang, H., Yang, X., Zhang, X., Li, Y., Fan, X., 2022. Role of pathogen-laden expiratory droplet dispersion and natural ventilation explaining a COVID-19 outbreak in a coach bus. Build. Environ. 220 https://doi.org/10.1016/j.buildenv.2022.109160.

Nair, A.N., Anand, P., George, A., Mondal, N., 2022. A review of strategies and their effectiveness in reducing indoor airborne transmission and improving indoor air quality. Environ. Res. 213 https://doi.org/10.1016/j.envres.2022.113579.

NCDC, 2022. Coronavirus Disease (COVID-2019) Situation Reports [WWW Document]. World Heal. Organ. URL. https://www.who.int/emergencies/diseases/novel-coronavirus-2019/situation-reports/.

O'Rourke, P.J., Amsden, A.A., 1987. The tab method for numerical calculation of spray droplet breakup. SAE Tech. Pap. https://doi.org/10.4271/872089.

Ong, S.W.X., Tan, Y.K., Chia, P.Y., Lee, T.H., Ng, O.T., Wong, M.S.Y., Marimuthu, K., 2020. Air, surface environmental, and personal protective equipment contamination by Severe Acute respiratory Syndrome coronavirus 2 (SARS-CoV-2) from a symptomatic patient. JAMA, J. Am. Med. Assoc. https://doi.org/10.1001/jama.2020.3227.

Passos, R.G., Silveira, M.B., Abrahão, J.S., 2021. Exploratory assessment of the occurrence of SARS-CoV-2 in aerosols in hospital facilities and public spaces of a metropolitan center in Brazil. Environ. Res. 195 https://doi.org/10.1016/j.envres.2021.110808.

Ranz, W.E., Marshall, W.R., 1952. Evaporation from drops 1. Chem. Eng. Prog. 48 (3), 141–146, 1952.

Santamaría Bertolín, L., Fernández Oro, J.M., Argüelles Díaz, K., Galdo Vega, M., Velarde-Suárez, S., Del Valle, M.E., Fernández, L.J., 2023. Optimal position of air purifiers in elevator cabins for the improvement of their ventilation effectiveness. J. Build. Eng. 63 https://doi.org/10.1016/j.jobe.2022.105466.

Spillman, J.J., 1984. Evaporation from freely falling droplets. Aeronaut. J. 88, 181–185. https://doi.org/10.1017/S0001924000020479.

Tellier, R., Li, Y., Cowling, B.J., Tang, J.W., 2019. Recognition of aerosol transmission of infectious agents: a commentary. BMC Infect. Dis. 191 (19), 1–9. https://doi.org/10.1186/S12879-019-3707-Y, 2019.

Wang, X., Yang, Y., Xu, Y., Wang, F., Zhang, Q., Huang, C., Shi, C., 2021. Prediction of vertical thermal stratification of large space buildings based on Block-Gebhart model: case studies of three typical hybrid ventilation scenarios. J. Build. Eng. 41 https://doi.org/10.1016/j.jobe.2021.102452.

Wells, W.F., 1933. ON AIR-BORNE INFECTION.* study II. Droplets and droplet nuclei. Under the title, "viability of bacteria in. t Stokes' Math. Phys. Pap. 1, 60.

Wiktorczyk-kapischke, N., Grudlewska-buda, K., Wa, E., Kwieci, J., Radtke, L., Gospodarek-komkowska, E., Skowron, K., 2021. Science of the total environment SARS-CoV-2 in the environment — non-droplet spreading routes. Sci. Total Environ. 770, 145260.

Xie, X., Li, Y., Chwang, A.T.Y., Ho, P.L., Seto, W.H., 2007. How far droplets can move in indoor environments - revisiting the Wells evaporation- falling curve. Indoor Air 17, 211–225. https://doi.org/10.1111/J.1600-0668.2007.00469.X.

Zhang, M., Wang, H., Foster, E.R., Nikolov, Z.L., Fernando, S.D., King, M.D., 2022. Binding behavior of spike protein and receptor binding domain of the SARS-CoV-2 virus at different environmental conditions. Sci. Rep. 12, 1–13. https://doi.org/10.1038/s41598-021-04673-y.

Zhou, Y., Ji, S., 2021. Experimental and numerical study on the transport of droplet aerosols generated by occupants in a fever clinic. Build. Environ. 187, 107402 https://doi.org/10.1016/j.buildenv.2020.107402.

Zou, Y., Zhao, X., Chen, Q., 2018. Comparison of STAR-CCM+ and ANSYS Fluent for simulating indoor airflows. Build. Simulat. 11, 165–174. https://doi.org/10.1007/s12273-017-0378-8.